Archives of Materials Science and Engineering

Volume 109
Issue 1
May 2021
Pages 5-16

International Scientific Journal
published monthly by the
World Academy of Materials
and Manufacturing Engineering

DOI: 10.5604/01.3001.0015.0510

Influence of hard segments content on thermal, morphological and mechanical properties of homo and co-polyurethanes: a comparative study

Z.K. Alobad [a,*], M. Albozahid [b], H.Z. Naji [c], H.S. Alraheem [d,e], A. Saiani [e]

[a] Department of Polymer Engineering and Petrochemical Industries,
Faculty of Materials Engineering, University of Babylon, Hilla, Iraq
[b] Department of Materials Engineering, Faculty of Engineering, University of Kufa, Najaf, Iraq
[c] Department of Chemical Engineering, Faculty of Engineering, University of Babylon, Hilla, Iraq
[d] Department of Ceramics and Building Materials Engineering,
Faculty of Materials Engineering, University of Babylon, Hilla, Iraq
[e] Department of Materials, The University of Manchester, Oxford Road M13 9PL, Manchester, UK
* Corresponding e-mail address: mat.zoalfokkar.alobad@uobabylon.edu.iq
ORCID identifier: https://orcid.org/0000-0002-1480-3432 (M.A.)

ABSTRACT

Purpose: This work aims to study the effect of hard segments (HS) content on the thermal, morphological and mechanical properties of polyurethane polymers based on 1.5 pentanediol chain extenders.

Design/methodology/approach: Two comparable series of polyurethanes were synthesised including homo-polyurethane (Homo-PU) and copolyurethane (Co-PU). The Homo-PU consists of 100% wt. of hard segments (HS). The Co-PU composes of 30%wt. of soft segments (SS) using a poly(ethylene glycol)-block-poly(propylene glycol)-block-poly(ethylene glycol) material. The effect of hard segments content on the morphology of Homo-PU and Co-PU was also studied.

Findings: The Homo-PU and Co-PU materials show three distinct degradation steps with the higher thermal stability of the Co-PU compared to the Homo-PU. Enthalpy of fusion (ΔH_M) and heat capacity (ΔC_P) of polyurethane (PU) samples decrease with decreasing HS content. In the cooling cycle, the higher exothermic peak of crystallization is observed in the Co-PU. In contrast, the cold crystalline peak is observed in the 2nd heating cycle of the Homo-PU. Melting temperature (T_M) increases with increasing SS content. Glass transition temperature (T_g) of PU samples shifts to higher temperature with increasing HS content. Storage modulus (E') of the Co-PU is higher than E' of the Homo-PU. All N-H groups in PU samples are hydrogen-bonded, whilst most of the C=O groups are hydrogen-bonded. The degree of hydrogen bonding in PU samples decreases with decreasing HS content. The Homo-PU shows better hardness than the Co-PU and higher brittleness at low temperature. WAXS results of the Homo-PU display better crystallinity compared to the Co-PU.

Research limitations/implications: The main challenge in this work was how to synthesis Thermoplastic polyurethanes (TPUs) with specific properties to compete other common polymer such as Polyamides (PA) and Polypropylene (PP).

Practical implications: Thermoplastic polyurethanes (TPUs) can be used in various application such as backageing, foot,automobiles and constructions.

Originality/value: A new type of TPUs that synthesized using different type of chain extender (1.5 pentanediol). Two different types of TPUs were synthesized one contained 30% SS and 70% HS and a second one contained 100% HS.

Keywords: Homo-polyurethane, Co-polyurethane, Polyurethane synthesis, Hard segments, Thermal, Morphological and mechanical properties

Reference to this paper should be given in the following way:

Z.K. Alobad, M. Albozahid, H.Z. Naji, H.S. Alraheem, A. Saiani, Influence of hard segments content on thermal, morphological and mechanical properties of homo and co-polyurethanes: a comparative study, Archives of Materials Science and Engineering 109/1 (2021) 5-16. DOI: https://doi.org/10.5604/01.3001.0015.0510

PROPERTIES

1. Introduction

Polyamides (PA) have been extensively used in a wide range of high-end engineering applications due to their high mechanical properties; nonetheless, their usage in engineering applications faced significant problems due to their high costs, high melting point during manufacturing, low toughness and high moisture absorption in service [1]. In the last decade, there were a swift increment in thermoplastics exploiting for industrial applications because of their low cost, high toughness, re-processability and recyclability [2,3]. Polypropylene (PP) is one of the most candidates for semi-crystalline thermoplastics polymer to use due to its low cost, lightweight, low melting point and high toughness [4]. However, High hard block content of Thermoplastic polyurethanes (TPUs) showed a combined effect of the low melting point as PP polymer and good mechanical properties as PA polymer. TPUs are linear block copolymers typically constructed of statistically alternating soft (SS) and hard (HS) segments [5]. As a result of significant interest in designing of TPUs with high HS content, ranging from 50 to 100% many researchers had an endeavour to use TPU with a high percent of HS [6-9]. Typically, the SS of TPUs consists from a polyether or polyester polyol, while the HS correspond to a diisocyanate chain extended using a diol or diamine. The reaction between the alcohol and amide groups results in the formation of urethanes/ureas linkages that can form hydrogen bonds [10,11]. TPUs characteized by a phase separated morphology resulting from the incompatibility between the SS and the HS resulting from the formation of a HS rich phase (HP) and SS rich phase (SP) [10,12]. The thermal, and mechanical properties of TPUs are affected by the microphase morphology formed depending on the exact chemical composition of the different segments and their ratio [10,11,13-16].

As forementioned , high HS content TPUs have attracted significant interest as they combine the low melting temperature of PP and the high mechanical properties of PA. In this type of materials, the choice of chain extended in the HS has a key influence on the properties of the materials. The short chain extended tend to lead to high modulus but brittle materials while long chain extenders tend to lead to low modulus but tough materials. In this work, we decide to investigate the properties of TPUs synthesized using 1.5 pentanediol chain extender. In current work, two types of TPUs were synthesized. The first one contained 30% SS and 70% HS and the second one contained 100% HS. The properties of these two TPUs were investigated via different techniques including DSC, TGA, DMTA, SEM, WAXS, FTIR and hardness.

2. Experimental section

2.1. Materials

The soft segment was used in the synthesizing of Co-PU polymers was Voranol EP 2010 polyol based on a polyethylene glycol-block-polypropylene glycol-block-polyethylene glycol structure (EO-PPO-EO) (supplied by Dow Chemicals) with a number average molecular weight ($\bar{M}_n$) 2000 g/mol and functionality 2.0. The hard segment was 4.4′-methylenebis phenyl isocyanate (MDI) chain extended with 1.5 pentanediol. 1.4-diazabicyclo [2.2.2]octane (DABCO-S) used as catalyst and N, N dimethyl-acetamide (DMAc) used as a solvent in the synthesising of PUs. All these chemicals were supplied by Sigma-Aldrich (UK).

2.2. Homo-PU and Co-PU synthesis

The Homo-PU used in this work was prepared by a one-step reaction process. The Homo-PU consists of 100% wt.

of hard segments. The hard segment was 4.4′-methylenebis phenyl isocyanate (MDI) chain extended with 1.5 pentanediol. On the other hand, a two-step reaction process was used to synthesis Co-PU. The Co-PU composes of 70% wt. of hard segments and 30%wt. of soft segments.

First step

The pre-polymer was prepared by the reaction of EO-PPO-EO and MDI at 80ºC in an oil bath under a nitrogen atmosphere, this reaction leading to polyol ended capping with MDI (see Figs. 1a and 2a). Other detailed synthesis procedure can be found in previous study [17].

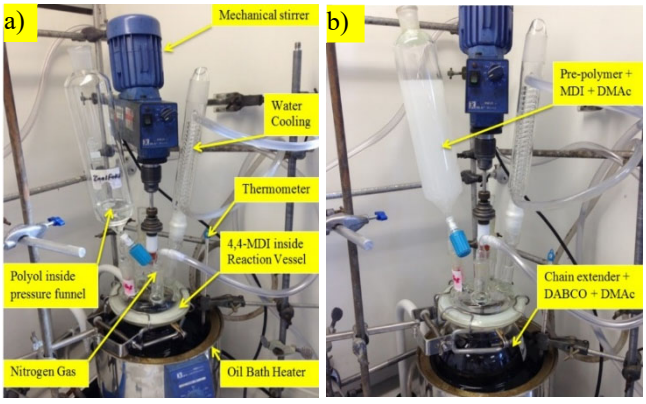

Fig. 1. (a) first step of the Co-PU-polymerisation process and (b) Homo-PU and second step of the Co-PU polymerisation process

Second step

The 1.5 pentanediol chain extender, 1.4-diazabicyclo [2.2.2]octane (DABCO-S) and N, N dimethyl-acetamide (DMAc) weighted were mixed in a dry reaction vessel (see Figs. 1b and 2b). Then, the vessel of the reaction was placed in the oil bath at 80ºC with a mechanical stirrer under nitrogen. On the other hand, MDI, DMAc and pre-polymer weighted were stirred together in a dry glass jar via a magnetic stirrer until the granules of MDI was dissolved. Following this, the mixture in the jar was poured into a pressure dropping funnel to drop for more than 20 minutes with continuous stirring into the reaction vessel, which had the mixture of the chain extender, DABCO-S and DMAc. After that, DMAc weighted was dropped into the reaction vessel. The final mixture was stirred continuously for 1.5 hours at 80ºC under nitrogen. At the end of this stage, hard segments were created by the reaction MDI with chain extender. The first and second steps were used to produce Co-PU. In contrast, it was used only the second step to produce Homo-PU with 100%wt. hard segment without attendance the polyol. The resulting solution (Co and Homo PU solution) was stored in sealed glass jars (see Fig. 3a) in dry conditions.

2.3. Solvent casting films

The solutions of Homo-PU and Co-PU with DMAc that were produced in PU synthesis were poured into the casting moulds made from a flat poly(tetrafluoroethylene) (see Fig. 3b).

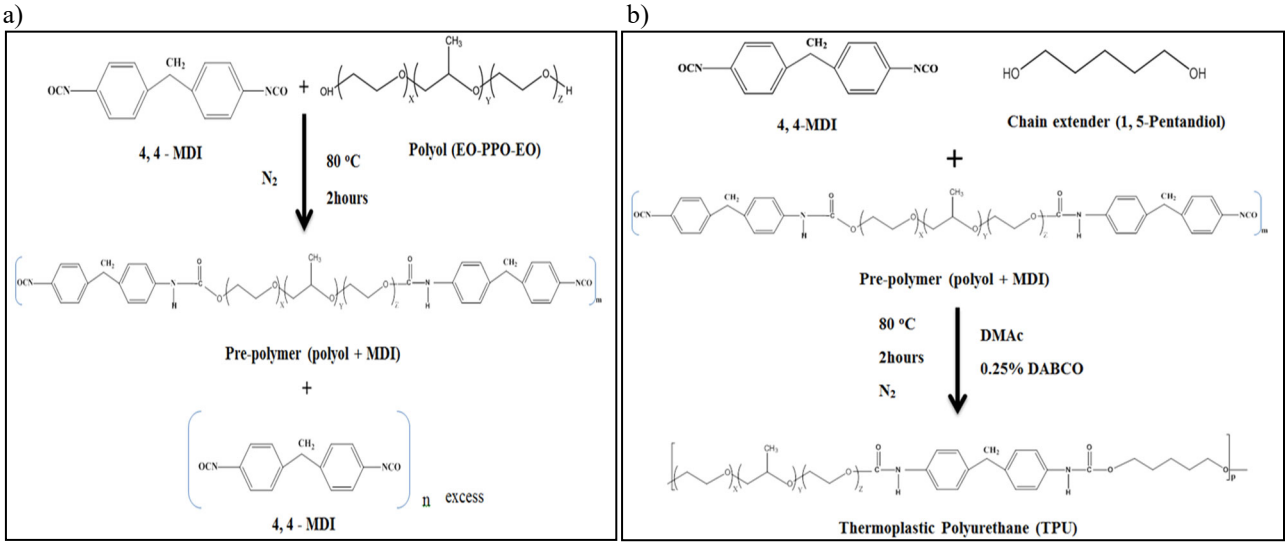

Fig. 2. (A) chemical reactions in the first step of the Co-PU-polymerisation process and (B) chemical reactions in the Homo-PU and second step of the Co-PU polymerisation process

a) b)

Fig. 3. a) PU solution in a glass jar after synthesis and b) solvent casting of PU films inside PTFE moulds

Following this, the moulds were placed into a pre-heated oven for 3 days at 80ºC under vacuum for 6 hours on the third day. After that, the casting Homo-PU and Co-PU films with approximately 1 mm thickness were carefully taken out from the moulds and kept in a desiccator to be used later.

2.4. Compression moulding process

Compression moulding was useful to prepare to flatten Homo-PU and Co-PU films, samples of Homo-PU and Co-PU. It can be in one stage for flattening Homo-PU and Co-PU samples or in two stages for Homo-PU and Co-PU.

First stage

Solvent casing moulding Homo-PU and Co-PU films were placed between release PTFE films. After that, they were put in a compression mould which was preheated at 170ºC, then it can be obtained flattened films of Homo-PU and Co-PU that were cooled to room temperature with approximately 0.2 mm thickness.

Second stage

Flattened Homo-PU and Co-PU films, which were produced in the first stage of compression moulding, which were cut the same size as the compression mould, put together into the pre-heated mould. The compression mould preheated to 180ºC. It was used 10 MPa as a compression pressure to compress the samples and they lasted in this pressure for about 3 minutes. Following this, the samples were cooled from compression temperature to room temperature using a water cooling system with a cooling rate of about 10ºC/min.

2.5. Characterization

Thermogravimetric Analysis (TGA)

TGA model Q500 with a sensitivity of weight of 0.1 µg was utilised to determine the thermal stability and decomposition of the Homo-PU and Co-PU samples. The weight of the samples studied in this work was in a range of 15-25 mg. Thermal degradations were investigated from ambient temperature to 1000ºC with a ramp rate of 10ºC/min. It can be defined as the decomposition temperature using the peak temperature of the derivative thermogravimetric (DTG) curve and on-set degradation temperature.

Differential Scanning Calorimetry (DSC)

DSC model Q100 (TA Instruments) was used to study the thermal transitions of the Homo-PU and Co-PU. The weight of the Homo-PU and Co-PU samples were (8-10 ±0.5 mg), and they were sealed into aluminium hermetic pans. The thermal protocol in Table 1 used is based on a sequence of heat/cool/heat. The Homo-PU and Co-PU samples were melted at 220ºC (about 40ºC more than the melting temperature of PUs).

Table 1.
Resume of the cycles of the thermal protocol of DSC

Cycle	Sequence	Isotherm time
Cycle 1	Cooling from 25 to -90ºC	3 min at -90ºC
Cycle 2	Heating 10ºC/min from -90 to 220ºC	3 min at 220ºC
Cycle 3	Cooling from 220 to -90ºC	3 min at -90ºC
Cycle 4	Heating 10ºC/min from -90 to 220ºC	3 min at 220ºC

Dynamic Mechanical Thermal Analysis (DMTA)

DMTA model Q800 (TA Instruments) was used to study the dynamic mechanical thermal properties of the Homo-PU and Co-PU depending on tension mode. The specimen dimensions of tension mode used were approximately 30 mm length, 8 mm width and less than 1 mm thickness. The test conditions used were a frequency of 1 Hz, the amplitude of 10 µm and a temperature ramp of (-120ºC to 150ºC) at a heating rate of 3ºC /min.

Fourier Transform Infrared Spectroscopy (FTIR)

FTIR model Thermo Nicolet 5700 with a Smart Orbit ATR, was used for this work. The wavenumbers that are operated by the single-reflection attenuated total reflectance (ATR) cell are from (400-4000 cm^{-1}). OMNIC software was

used to analyse the data, and H-bonding in PU films can be determined by normalising all spectra to make the lowest absorbance reaches zero intensity.

Hardness

It was used hardness-meter Shore-D tester" TH210 (Time Group Inc.) to measure the hardness of the Homo-PU and Co-PU according to ASTM D2240-02 test method. It was recorded 10 readings in different places at room temperature for each specimen.

Wide-Angle X-ray Scattering (WAXS)

WAXS experiments were carried out for Homo-PU and Co-PU matrices using a D8 advance Bruker X-ray. A fixed copper K-alpha target was used, and the operating conditions of the test were 40 mA and 40 kV. The scanning speed and step size utilised were 0.05°/6 s and 0.05°, respectively. The scanning 2θ range was between 4°-70°, and the dimensions of the Homo-PU and Co-PU samples were cut from random specimens with a size of 1.5 cm × 1.5 cm. 3 specimens of each sample were tested.

Scanning Electron Microscopy (SEM)

SEM model a Phillips XL 30 FEG was used in this project. The Homo-PU and Co-PU samples were broken to investigate their freeze-fracture surfaces after they were dipped in liquid nitrogen. It was used 12.5 mm aluminium pin stubs as sample holders and was used double-sided adhesive carbon discs to fix samples onto the holders. Besides, the space between samples and holders was filled with silver paint as a conductive path to prevent electron accumulation on the sample surfaces. Following this, gold was coated onto the sample surface using an Edwards Sputter Coater S150B. It was used secondary electron imaging and the accelerating voltage of the electron beam was set at 10 kV for characterisation of Homo-PU and Co-PU samples.

3. Results and discussion

3.1. Thermal stability

Thermal degradation of PUs includes many reactions which happen during the heating process. The thermal stability of PUs is strongly dependent on the raw materials [18]. In Figure 4a, the Co-PU samples show higher onsets' temperature than the Homo-PU samples. The onsets' temperature of the Co-PU and Homo-PU is at 326 ± 0.55°C and 312 ± 0.5°C, respectively. This can be attributed to the Homo-PU has 100%wt. of HS without any SS [19]. Besides, the weight loss of the Co-PU and Homo-PU is 88 ± 0.8% and 91 ± 1%, respectively. In Figure 4b, thermoplastic PUs generally show four distinct degradation steps [10]. The Co-PU displays three distinct degradation steps as shown in maximum peaks (268 ± 0.6, 335 ± 0.9, 363 ± 1.1 and 544 ± 0.5°C). As such, three degradation steps are observed in the Homo-PU as seen in maximum peaks (244 ± 0.3, 329 ± 0.36 and 551 ± 0.2°C). The first degradation step is only observed in the Homo-PU due to higher hard segments (HS) content. This step is associated with comparatively low weight loss and related to the start of degradation of the urethane bonds in the PU samples resulting in carbon dioxide [18].

a)

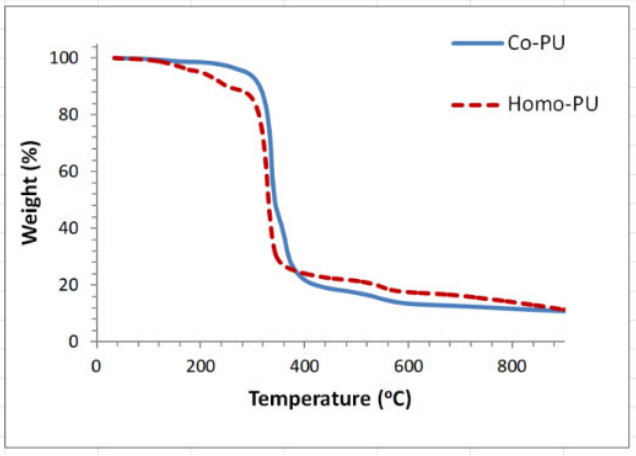

b)

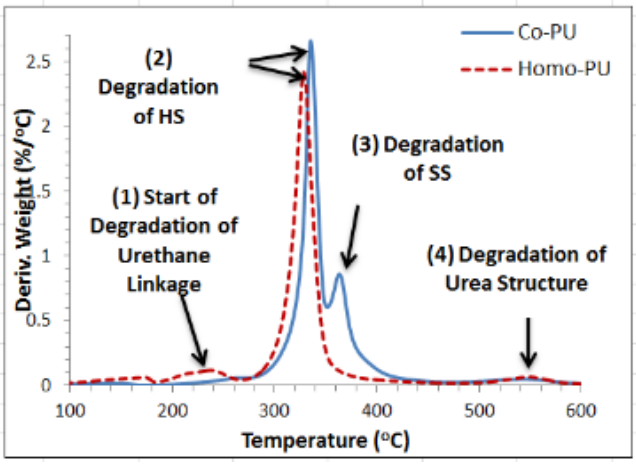

Fig. 4. a) TGA curves and b) first derivative of the weight loss vs temperature (DTG) curves of the Homo-PU and Co-PU

The second (major) degradation step represents the most weight loss of PU samples. The second degradation step is seen in the Homo-PU and Co-PU samples. The degradation in this step is attributed to the degradation (decomposition) of the HS in the PU samples [9-11]. The degradation of HS

includes the decomposition of urethane bonds, leading to the presence of alcohol and isocyanate groups. Following this, isocyanate groups dimerised to produce carbodiimides which react with free alcohol groups resulting in the formation of thermally stable substituted urea [10,11]. The second degradation step of the Homo-PU samples is less intensity, and shifts to lower temperatures. This is due to the first step of degradation reducing the weight fraction of the HS in the second degradation step. The third degradation step is only visible in the Co-PU as a higher temperature shoulder to the second (major) degradation step. The degradation in this step is due to the degradation (decomposition) of the SS in the Co-PU [10]. The fourth step with a comparatively low weight loss is observed in the Homo-PU and Co-PU samples. This step of degradation relates to the degradation of thermally stable substituted urea structure which was produced in the previous degradation step resulting in the volatiles and carbonaceous char [9-11]. The Co-PU samples display greater thermal stability than the Homo-PU samples due to the presence of the SS in the Co-PU [19].

3.2. Thermal transitions

Figure 5a shows the thermal transitions of the Homo-PU and Co-PU in the first heating cycle. Both T_g of the SP (T_{gSP}) of the Co-PU and T_g of the HP (T_{gHP}) of the Homo-PU and Co-PU are visible as presented in Table 2. The T_{gHP} of the Homo-PU and Co-PU are at 54.5 ± 1.6ºC and 45 ± 3.1ºC, respectively. The Homo-PU displays higher T_{gHP} than the Co-PU. While the T_{gSP} of the Co-PU is at -34 ± 3.1ºC. It is observed that the T_M of PU samples is around 177ºC. The change in enthalpy of fusion (ΔH_M) increases with increasing the HS content. The Homo-PU samples present higher ΔH_M than the Co-PU samples (see Fig. 5 and Table 2). With increasing the HS content, the crystallinity and ΔH_M of the PU samples are enhanced in agreement with previous works [20-22]. A. A. Tsiotas [10] reported that PUs with 65%-95% wt. of HS in the first heating cycle had a T_M between 169 ºC and 173ºC and an ΔH_M between 24 J/g and 44 J/g. An increase in the HS content results in an improvement in the order of HS domains (crystallisation of HS), leading to enhancement in the interaction among PU chains [20-24]. As a result, 100%wt. of the HS encourages the formation of HS domains with more than 65%wt. of the HS, resulting in high crystallinity and ΔH_M of the Homo-PU samples.

The first cooling DSC thermographs of the Homo-PU and Co-PU samples are displayed in Figure 5b. The results display that the T_{gHP} of the PU samples is around 75ºC. Heat capacity of the T_{gHP} (ΔC_{PHP}) increases with increasing the

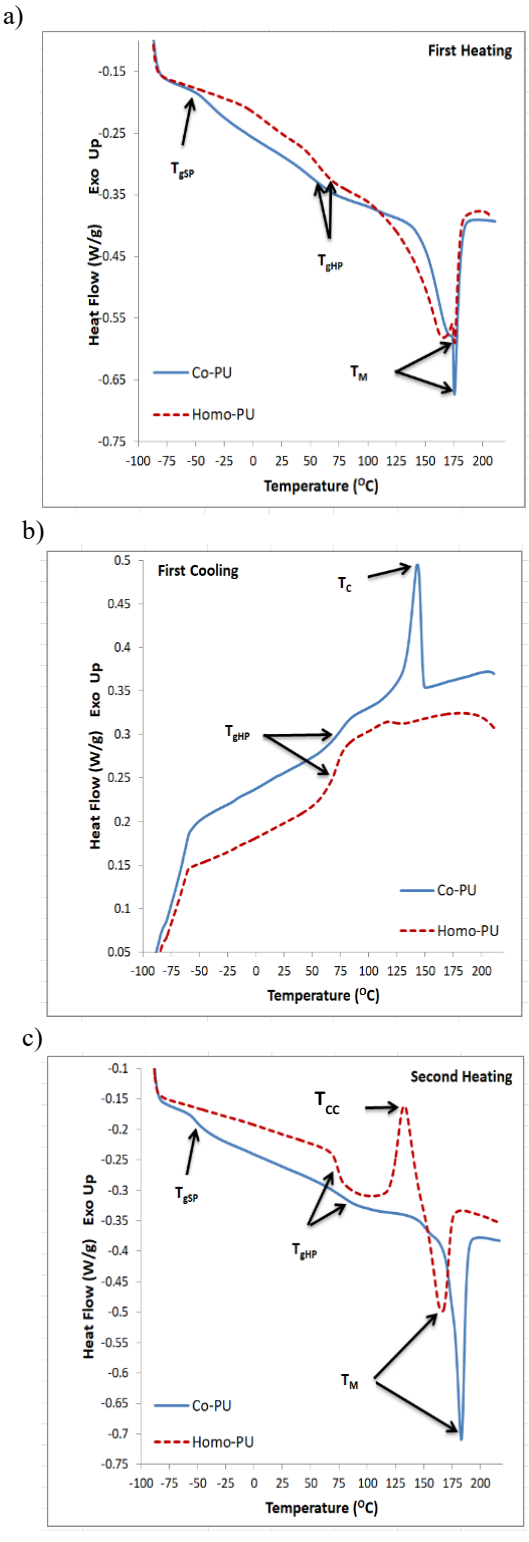

Fig. 5. DSC curves a) first heating cycle, b) first cooling cycle and c) second heating cycle of the Homo-PU and Co-PU with heating rate: 10ºC/min

Table 2.
Thermal Transitions of the Homo-PU and Co-PU samples

	Sample	Co-PU			Homo-PU		
		First Heating	First Cooling	Second Heating	First Heating	First Cooling	Second Heating
1	T_{gSP}, ºC	- 34±3.1	-	- 52.2±0.2	-	-	-
2	ΔC_{PSP}, J/g ºC	0.15±0.02	-	0.14±0.06	-	-	-
3	T_{gHP}, ºC	45±3.1	76±0.6	83±2.1	54.5±1.6	74±1.1	79±2.1
4	ΔC_{PHP}, J/g ºC	0.26±0.03	- 0.2±0.07	0.22±0.04	0.27±0.07	- 0.37±0.2	0.36±0.06
5	T_C, ºC	-	142±2.1	-	-	118.6±1	137±3.1
6	ΔH_C, J/g	-	19.9±2.1	-	-	0.14±0.34	14.7±0.4
7	T_M, ºC	177.3±1	-	184.5±0.6	177±5.1	-	168.5±1.6
8	ΔH_M, J/g	27.8±1.1	-	21.1±4.1	41.1±5.1	-	14.1±1.1

HS content of the PU samples at the same transition temperature ranges [10]. The exothermic peak of crystallization (T_C) is detected in the Co-PU at 142 ± 2.1ºC and Homo-PU at 118.6 ± 1ºC. The Co-PU samples show higher enthalpy of crystallisation (ΔH_C) and T_C than the Homo-PU samples. This is because the exothermic peak of the Co-PU connected to the available mobility of the SS and HS in the Co-PU structure upon cooling. As such, 30% wt. of SS assists in the mobility of HS to make crystalline HS domains in the Co-PU structure. As a result, mobility restrictions might be the major reason to prevent crystallization in the Homo-PU [8,9,19].

The second heating cycle was shown in Figure 5c and Table 2, the Co-PU displays slightly higher T_{gHP} than the Homo-PU, but the ΔC_{PHP} of the Co-PU is still lower than the Homo-PU. A. A. Tsiotas [10] reported that the T_{gHP} of PUs with hard segments 65%-95% in the second heating cycle was between 65ºC and 72ºC [10]. This indicates that the mobility of the SS and HS in the Co-PU is greater than the mobility of the HS in the Homo-PU. As such, the T_{gSP} of the Co-PU decreases from -34 ± 3.1ºC in the first heating cycle to -52.1 ± 0.2ºC in the second heating cycle. In contrast, the T_{gHP} of the Co-PU increases from 45 ± 3.1ºC in the first heating cycle to 83 ± 2.1ºC in the second heating cycle. This is because, in the first heating cycle, the de-mixing of the small islands of the mixed-phase based on SS and HS occurs, and in the cooling cycle the mobility of SS is less restricted by HS that are aggregated as crystalline HS domains in pure HP resulting in high phase separation (phase-separated mesophase) [10,24]. Also, the T_{gHP} of the Homo-PU in the second heating is higher than in the first heating due to de-mixing of mixed-phase based on crystalline and amorphous HS in pure HP.

In the second heating cycle, the Co-PU shows higher T_M than the Homo-PU because of the presence of the SS in the structure of the Co-PU. In contrast, ΔH_M increases with increasing HS content [12]. Cold crystalline peak (T_{CC}) at 137 ± 3.1ºC is only observed in the Homo-PU. This exothermic transition occurs when the semi-crystalline polymer is quenched (cooled) from the melting state into the highly amorphous state. The HS of the Homo-PU did not have enough time to crystallise during the cooling cycle [21].

3.3. Dynamic mechanical thermal properties

In Figure 6a, the storage modulus (E') of the Homo-PU and Co-PU decreases considerably with increasing the temperature and then suddenly drops at the glass transition temperature (T_g). The decrease in modulus is attributed to the thermal transition (T_g) from a glassy phase to a rubbery phase. It is seen that T_{gHP} region moves to a higher temperature and sharply changes with high HS content [8,14,15]. Although the E' value of the PU samples increases with increasing the HS content, the E' of the Homo-PU is lower than of the Co-PU. This is because of the Homo-PU composes of 100%wt. of HS resulting in high brittleness and micro-cracks which promote a reduction in storage modulus (tensile mode).

Figure 6b illustrates the difference in tan delta (δ) with temperature for the Homo-PU and Co-PU samples. It is observed that the T_g of the Homo-PU is higher than the T_g of the Co-PU. This is because the Homo-PU has higher hard segments content than the Co-PU. The results show that the temperature of the tan delta peak represents the T_g [14,25]. Two loss peaks are seen in the Homo-PU samples, including a secondary relaxation at about -76 to -81ºC and the T_{gHP} at about 56 to 62ºC. In contrast, one loss peak is seen in the Co-PU samples at about 3-6ºC including the T_g of mixed-phase (T_{gMP}). The second relaxation corresponds to rotational mechanisms (crankshaft rotation) occurring for (-CH_2-) groups in chain extender [11,15,16]. The tan delta peak of the PU samples shifts to higher temperature with increasing the HS content [8,14,15,20,26]. Furthermore, the intensity of the tan δ of the PU samples grows with increasing the HS content [8,15,23].

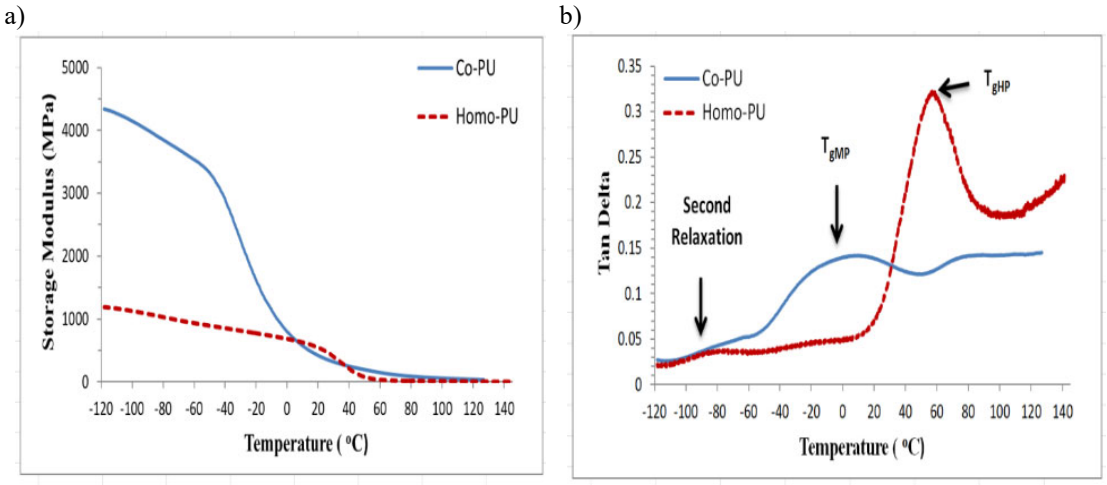

Fig. 6. Dynamic Mechanical Thermal data of a) Storage modulus, b) Tan delta (tensile mode) of the Homo-PU and Co-PU

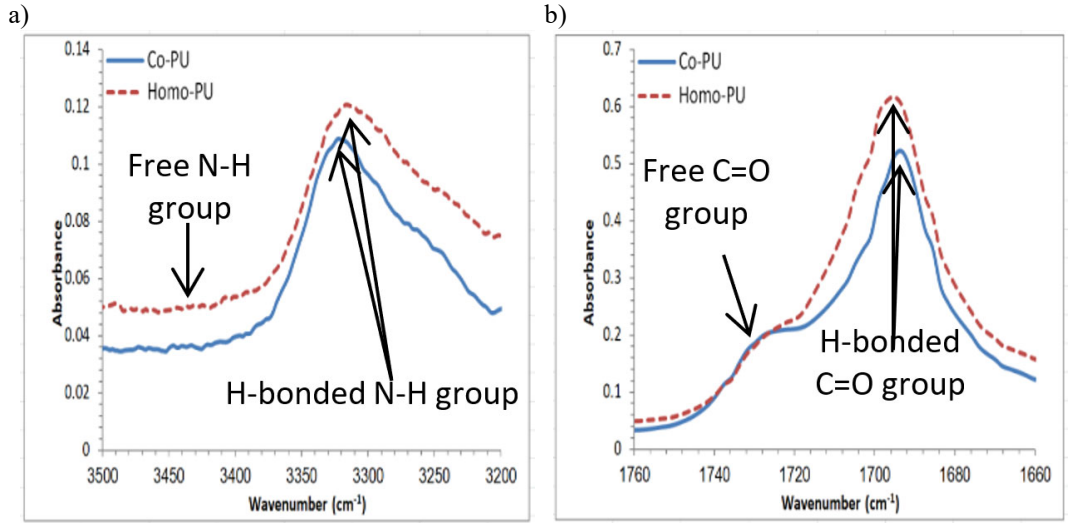

Fig. 7. ATR-FTIR spectra of (A) free N-H stretching and hydrogen-bonded N-H stretching and (B) free C=O stretching and hydrogen-bonded C=O stretching of the Homo-PU and Co-PU samples

This could be attributed to the volume of disordered and ordered HS and increases with increasing the HS content [23]. For this reason, the loss peak of the T_{gHP} of the Homo-PU samples is large and sharp and moves to a higher temperature. While the loss peak of the T_{gSP} and T_{gHP} of the Co-PU samples disappears due to the presence of the mixed-phase that composes of SS and HS in the Co-PU structure.

3.4. Hydrogen bonding in Homo-PU and Co-PU

Figure 7a shows free (non-hydrogen bonded) and hydrogen-bonded N-H stretching regions of the Homo-PU and Co-PU samples. The NH stretching region is from 3200 cm^{-1} to 3500 cm^{-1} for all samples. The hydrogen-bonded N-H band is observed in the Co-PU samples at 3321-3323 cm^{-1} and in the Homo-PU at 3315-3318 cm^{-1}. The graph displays that all N-H groups are hydrogen-bonded as the proton donor in agreement with previous works [11,27].

Figure 7b displays the free and hydrogen-bonded C=O stretching regions of the Homo-PU and Co-PU samples. The C=O stretching region of the PU samples is from 1660 to 1760 cm^{-1}. Two bands are overlapping including a free C=O band and a hydrogen-bonded C=O band. A weakly free C=O band centred is at 1724-1727 cm^{-1} for all samples, while

a strong hydrogen-bonded C=O band centred is at 1693-1694 cm^{-1} and 1695-1696 cm^{-1} for the Co-PU and the Homo-PU samples, respectively. This is attributed to the hydrogen bonding between HS - HS in the Homo-PU, and between HS-HS, and HS-SS in the Co-PU. Besides, not all N-H groups in the HS of the Co-PU hydrogen-bonded with C=O group in the HS, but some of them may be hydrogen-bonded with urethane alkoxy oxygen, N-H groups and oxygen of an ether group (C-O-C). In contrast, some of the N-H groups in the HS of the Homo-PU might be hydrogen-bonded with urethane alkoxy oxygen and N-H groups [28,29].

3.5. Hardness of Homo-PU and Co-PU

The hardness of PU samples increases with increasing HS content (see Fig. 8). As such, the Co-PU shows lower hardness than the Homo-PU. The hardness shore-D of the Homo-PU is 83.7 compared with the hardness shore-D of the Co-PU is 63.6 due to the Co-PU has 30%wt. of SS.

3.6. Wide-angle X-rays results

WAXS diffractograms of Homo-PU and Co-PU are presented in Figure 9. The results show that Bragg diffraction peaks are seen in all polyurethane samples at 21° and 43°. These peaks show a degree of ordering in the hard segment domains (crystallisation) of Homo-PU and Co-PU samples. The volume of crystallinity is represented as an area under the Bragg diffraction peaks [10,23], and it is affected by hard segments content. An increase of the area under the Bragg diffraction peaks of the WAXS graph as a result of increasing hard segments content [23] (see Fig. 9). Homo-PU samples display the greatest volume of crystalline phase in agreement with the DSC results. The degree of ordering in the hard segments domains (crystallisation) of polyurethane samples increases with increasing hard segments content, resulting in improvement in the interaction among polyurethane chains. Hence, the formation of ordered hard segments domains is encouraged by the 100%wt. hard segments more than by 70%wt. hard segments.

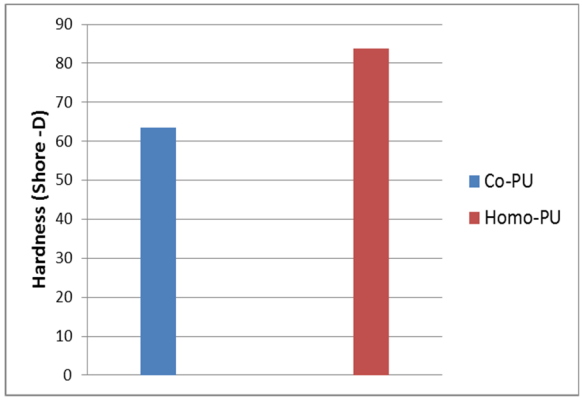

Fig. 8. Hardness (Shore-D) of the Co-PU and Homo-PU

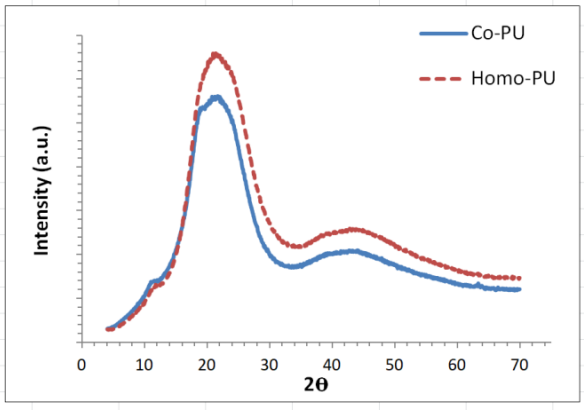

Fig. 9. Wide-angle X-rays with the scattered intensity of Homo-PU and Co-PU

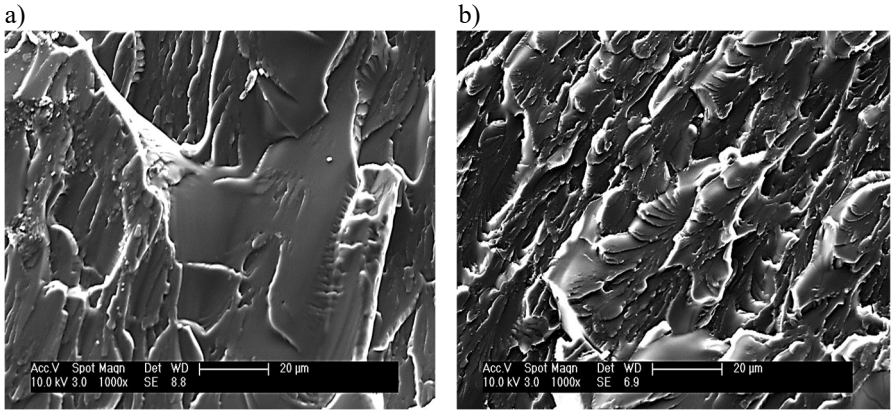

Fig. 10. Scanning electron micrographs of: a) Co-PU and b) Homo-PU

3.7. Morphology of Homo-PU and Co-PU matrices

In Figure 10 (a and b), Homo-PU shows higher brittleness than Co-PU at low temperature. The surface of Homo-PU has bigger hackles and is rougher than Co-PU that does not have the same phenomenon. It can be attributed to Homo-PU has higher hard segments content than Co-PU, leading to greater brittleness. In other words, Co-PU displays good flexible properties at low temperatures due to having 30% wt. of soft segments in its structure.

4. Conclusions

Three steps of degradation are observed in the Co-PU and Homo-PU. The Co-PU shows higher thermal stability than the Homo-PU. The ΔH_M and ΔC_P decrease with increasing the SS content. In the cooling cycle, the exothermic peak of crystallization of the Co-PU is higher than of the Homo-PU. Phase separation in the Co-PU is in the second heating cycle higher than in the 1st heating cycle. The cold crystalline peak is observed in the Homo-PU in the second heating cycle. In the second heating cycle, the value of T_M increases with increasing the SS of the Co-PU samples. T_g of Co-PU samples shifts to lower temperature with increasing SS content.

The Co-PU shows higher E' than the Homo-PU. It is observed two loss peaks; a second relaxation and T_{gHP} in the Homo-PU and one loss peak T_{gMP} in the Co-PU. All N-H groups are hydrogen-bonded, whilst most of C=O groups are hydrogen-bonded. In WAXS results, Co-PU samples display lower crystallinity than Homo-PU samples. Homo-PU has higher brittleness and lower flexibility at low temperature than Co-PU. The Co-PU has higher flexibility at low temperature, phase separation, storage modulus, T_M and thermal stability than the Homo-PU. The homo-PU displays higher crystallinity, hardness, T_g than the Co-PU.

Acknowledgements

The authors are gratefully acknowledge the financial support from the Iraqi Ministry of Higher Education and Scientific Research of Iraq and the University of Babylon (Scholarship Grant No. 937).

References

[1] S.C. Tjong, S.A. Xu, R.K.-Y. Li, Y.W. Mai, Short glass fiber-reinforced polyamide 6,6 composites toughened with maleated SEBS, Composites Science and Technology 62/15 (2002) 2017-2027. DOI: https://doi.org/10.1016/S0266-3538(02)00140-9

[2] H. Wittich, M. Evstatiev, E. Bozwelieva, K. Friedrich, S. Fakirov, Effect of crystallinity on the interlaminar fracture toughness of continuous glass fiber-polyamide composites, Advanced Composite Materials 2/2 (1992) 135-152. DOI: https://doi.org/10.1163/156855192X00161

[3] J.H. Chen, E. Schulz, J. Bohse, G. Hinrichsen, Effect of fibre content on the interlaminar fracture toughness of unidirectional glass-fibre/polyamide composite, Composites Part A: Applied Science and Manufacturing 30/6 (1999) 747-755. DOI: https://doi.org/10.1016/S1359-835X(98)00188-2

[4] Y. Mi, X. Chen, Q. Guo, Bamboo fiber-reinforced polypropylene composites: Crystallization and interfacial morphology, Journal of Applied Polymer Science 64/7 (1997) 1267-1273. DOI: https://doi.org/10.1002/(SICI)1097-4628(19970516)64:7%3C1267::AID-APP4%3E3.0.CO;2-H

[5] M. Albozahid, H.Z. Naji, Z.K. Alobad, A. Saiani, Effect of OMMT reinforcement on morphology and rheology properties of polyurethane copolymer nanocomposites, Journal of Elastomers and Plastics (2021) 1-23 (published online). DOI: https://doi.org/10.1177%2F00952443211006160

[6] K. Kojio, M. Furukawa, S. Motokucho, M. Shimada, M. Sakai, Structure-mechanical property relationships for poly(carbonate urethane) elastomers with novel soft segments, Macromolecules 42/21 (2009) 8322-8327. DOI: https://doi.org/10.1021/ma901317t

[7] L.S.T.J. Korley, B.D. Pate, E.L. Thomas, P.T. Hammond, Effect of the degree of soft and hard segment ordering on the morphology and mechanical behavior of semicrystalline segmented polyurethanes, Polymer 47/9 (2006) 3073-3082. DOI: https://doi.org/10.1016/j.polymer.2006.02.093

[8] B.S. Lee, B.C. Chun, Y. Chung, K. Il Sul, J.W. Cho, Structure and Thermomechanical Properties of Polyurethane Block Copolymers with Shape Memory Effect, Macromolecules 34/18 (2001) 6431-6437. DOI: https://doi.org/10.1021/ma001842l

[9] S.-H. Kang, D.-C. Ku, J.-H. Lim, Y.-K. Yang, N.-S. Kwak, T.-S. Hwang, Characterization for Pyrolysis of Thermoplastic Polyurethane by Thermal Analyses, Macromolecular Research 13/3 (2005) 212-217. DOI: https://doi.org/10.1007/BF03219054

[10] A.A. Tsiotas, The role of the chain extender on the phase behaviour and morphology of high hard block

content thermoplastic polyurethanes: Thermodynamics – Structures – Properties, PhD Thesis, University of Manchester, Manchester, UK, 2012.

[11] Z.-J. Wang, D.-J. Kwon, G.-Y. Gu, H.-S. Kim, D.-S. Kim, C.-S. Lee, K.L. DeVries, J.-M. Park, Mechanical and interfacial evaluation of CNT/polypropylene composites and monitoring of damage using electrical resistance measurements, Composites Science and Technology 81 (2013) 69-75. DOI: https://doi.org/10.1016/j.compscitech.2013.04.001

[12] D. Braun, H. Cherdron, M. Rehahn, H. Ritter, B. Voit, Polymer Synthesis: Theory and Practice Fundamentals, Methods, Experiments, 4th Edition, Springer–Verlag, Berlin–Heidelberg–New York, 2005. DOI: https://doi.org/10.1007/978-3-642-28980-4

[13] C.S. Paik Sung, C.B. Hu, C.S. Wu, Properties of Segmented Poly(urethaneureas) Based on 2,4-Toluene Diisocyanate. 1. Thermal Transitions, X-ray Studies, and Comparison with Segmented Poly(urethanes), Macromolecules 13/1 (1980) 111-116. DOI: https://doi.org/10.1021/ma60073a022

[14] C.G. Seefried, J.V. Koleske, F.E. Critchfield, Thermoplastic urethane elastomers. III. Effects of variations in isocyanate structure, Journal of Applied Polymer Science 19/12 (1975) 3185-3191. DOI: https://doi.org/10.1002/app.1975.070191204

[15] C.G. Seefried, J.V. Koleske, F.E. Critchfield, Thermoplastic urethane elastomers. II. Effects of variations in hard-segment concentration, Journal of Applied Polymer Science 19/9 (1975) 2503-2513. DOI: https://doi.org/10.1002/app.1975.070190913

[16] D.S. Huh, S.L. Cooper, Dynamic mechanical properties of polyurethane block polymers, Polymer Engineering and Science 11/5 (1971) 369-376. DOI: https://doi.org/10.1002/pen.760110504

[17] M. Albozahid, S.A. Habeeb, N.A.I. Alhilo, A. Saiani, The impact of graphene nanofiller loading on the morphology and rheology behaviour of highly rigid polyurethane copolymer, Materials Research Express 7/12 (2020) 125304. DOI: https://doi.org/10.1088/2053-1591/aba5ce

[18] M.Herrera, G. Matuschek, A. Kettrup, Thermal degradation of thermoplastic polyurethane elastomers (TPU) based on MDI, Polymer Degradation and Stability 78/2 (2002) 323-331. DOI: https://doi.org/10.1016/S0141-3910(02)00181-7

[19] C. Nedolisa, Designing High Hard Block Content Thermoplastic Polyurethane (TPU) Resins for Composite Applications, PhD Thesis, University of Manchester, Manchester, UK, 2015.

[20] L. Rueda-Larraz, B.F. D'Arlas, A. Tercjak, A. Ribes, I. Mondragon, A. Eceiza, Synthesis and microstructure-mechanical property relationships of segmented polyurethanes based on a PCL-PTHF-PCL block copolymer as soft segment, European Polymer Journal 45/7 (2009) 2096-2109. DOI: https://doi.org/10.1016/j.eurpolymj.2009.03.013

[21] R.G.J.C. Heijkants, R.V. van Calck, T.G. van Tienen, J.H. de Groot, P. Buma, A.J. Pennings, R.P.H. Veth, A.J. Schouten, Uncatalyzed synthesis, thermal and mechanical properties of polyurethanes based on poly(caprolactone) and 1,4-butane diisocyanate with uniform hard segment, Biomaterials 26/20 (2005) 4219-4228. DOI: https://doi.org/10.1016/j.biomaterials.2004.11.005

[22] A. Saiani, W.A. Daunch, H. Verbeke, J. Leenslag, J.S. Higgins, Origin of Multiple Melting Endotherms in a High Hard Block Content Polyurethane. 1. Thermodynamic Investigation, Macromolecules 34/26 (2001) 9059-9068. DOI: https://doi.org/10.1021/ma0105993

[23] A. Saralegi, L. Rueda, B. Fernández-D'Arlas, I. Mondragon, A. Eceiza, M.A. Corcuera, Thermoplastic polyurethanes from renewable resources: Effect of soft segment chemical structure and molecular weight on morphology and final properties, Polymer International 62/1 (2013) 106-115. DOI: https://doi.org/10.1002/pi.4330

[24] A. Saiani, C. Rochas, G. Eeckhaut, W.A. Daunch, X.J. Leenslag, J.S. Higgins, Origin of Multiple Melting Endotherms in a High Hard Block Content Polyurethane. 2. Structural Investigation, Macromolecules 37/4 (2004) 1411-1421. DOI: https://doi.org/10.1021/ma034604+

[25] J.P. Latere Dwan'isa, A.K. Mohanty, M. Misra, L.T. Drzal, M. Kazemizadeh, Biobased polyurethane and its composite with glass fiber, Journal of Materials Science 39/6 (2004) 2081-2087. DOI: https://doi.org/10.1023/B:JMSC.0000017770.55430.fb

[26] B.K. Kim, Y.J. Shin, S.M. Cho, H.M. Jeong, Shape-memory behavior of segmented polyurethanes with an amorphous reversible phase: the effect of block length and content, Journal of Polymer Science. Part B: Polymer Physics 38/20 (2000) 2652-2657. DOI: https://doi.org/10.1002/1099-0488(20001015)38:20%3C2652::AID-POLB50%3E3.0.CO;2-3

[27] R.W. Seymour, G.M. Estes, S.L. Cooper, Infrared Studies of Segmented Polyurethan Elastomers. I. Hydrogen Bonding, Macromolecules 3/5 (1970) 579-583. DOI: https://doi.org/10.1021/ma60017a021

[28] J. Bandekar, S. Klima, FT-IR spectroscopic studies of polyurethanes – Part II. Ab initio quantum chemical studies of the relative strengths of 'carbonyl' and 'ether' hydrogen-bonds in polyurethanes, Spectrochimica Acta Part A: Molecular Spectroscopy 48/10 (1992) 1363-1370. DOI: https://doi.org/10.1016/0584-8539(92)80142-J

[29] Z. Ren, D. Ma, X. Yang, H-bond and conformations of donors and acceptors in model polyether based polyurethanes, Polymer 44/20 (2003) 6419-6425. DOI: https://doi.org/10.1016/S0032-3861(03)00726-2